arXiv:hep-lat/9311008v1 4 Nov 1993

Geometric Measurement of Topological Susceptibility on Large Lattices*

J. Grandy and R. Gupta[a]

[a]T-8 Group, MS B285, Los Alamos National Laboratory, Los Alamos, New Mexico 87545 U. S. A.

The topological susceptibility of the quenched QCD vacuum is measured on large lattices for three β values from 6.0 to 6.4. Charges possibly induced by $O(a)$ dislocations are identified and shown to have little effect on the measured susceptibility. As β increases, fewer such questionable charges are found. Scaling is checked by examining the ratios of the susceptibility to three physical observables computed in Refs. [1, 2, 3, 4] and Λ_{latt}.

The topological susceptibility of the QCD vacuum is defined by

$$\chi_t = \langle Q^2 \rangle / V, \quad Q = \frac{-1}{16\pi^2} \int_V d^4x \, F(x) \tilde{F}(x) \ . \quad (1)$$

The susceptibility is related to the η' and η masses in the chiral large-N_c limit through the Witten-Veneziano formula[5]

$$\chi_t = \frac{f_\pi^2}{6}(m_{\eta'}^2 + m_\eta^2 - 2m_K^2) = (180 MeV)^4 \ . \quad (2)$$

The computation of χ_t on a lattice is not straightforward. The simplest method, replacing $F\tilde{F}$ by a product of plaquettes, suffers mixing with F^2 and a constant[6], and a large perturbatively determined renormalization factor, but cooling and smearing algorithms have been proposed to refine this method[7, 8]. The geometric method, first proposed by Lüscher[9], is not susceptible to multiplicative renormalization but contains additive divergences from compact dislocations[10] so that

$$\chi_t^{measured} = \chi_t + \int_{p_0}^{\infty} dp \, C(p) \, a^p \ . \quad (3)$$

The dislocation described by Göckeler *et al.*[11] produces a power $p_0 < 0$ in (3) and thus a power law divergence in the measured susceptibility as $a \to 0$. The factor $C(p)$ for $p < 0$ is crucial to determining the onset of divergent behavior in the measured susceptibility for finite a, and we investigate whether divergent terms affect the result at realistic values of a used in our calculation.

We are examining several aspects of topology on the lattice. First, we compute χ_t using the geometric method and examine the systematic effect of dislocations in the range $\beta = 6.0$ to $\beta = 6.4$. We plan to study the various methods of measuring χ_t, including cooling, and use the geometric topological charge density to examine the spin asymmetry in deep inelastic scattering off a proton. At present we have completed the first stage and report the results here.

Our lattice ensembles are listed in Table 1. We evaluate the integrals derived by Göckeler *et al.*[12] on the surfaces of each hypercube on the lattice, obtaining a local integer for each hypercube, and add the local integers in each configuration to obtain the topological charge Q. The integration requires a two-stage process. First, all hypercubes are integrated using two different coarse ($\sim 5^3$) cubic meshes. Hypercubes which show no definite evidence of convergence toward zero are integrated more accurately, with $\sim 10^3$ meshes on subcubes. Most hypercubes are brought within 10^{-4} to 10^{-5} of an integer with the finer mesh, but a few difficult hypercubes require further refinement. The number of difficult hypercubes per unit topological charge decreases as β increases.

We attempt to separate spurious charges, caused by low-action dislocations, from physical charges. These dislocations in $SU(2)$ typically contain a central plaquette near -1 and have a radius of about 1 lattice spacing[11]. Since the topological structure of $SU(3)$ is determined by

*Presented by J. Grandy. Work supported by University of California under DOE Contract W-7405-ENG-36. Computer time on C90 provided by NERSC and PSC Supercomputing Centers.

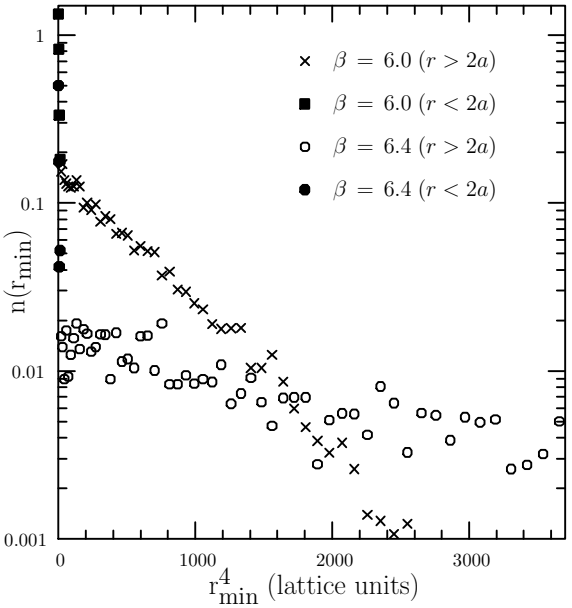

Figure 1. Normalized nearest neighbor correlations from charged hypercubes to nearest plaquette with $RDC < 0.15$ (Eq. 4), versus r^4_{min} in lattice units. Highlighted correlations at $r_{min} < 2a$ indicate possible compact dislocations.

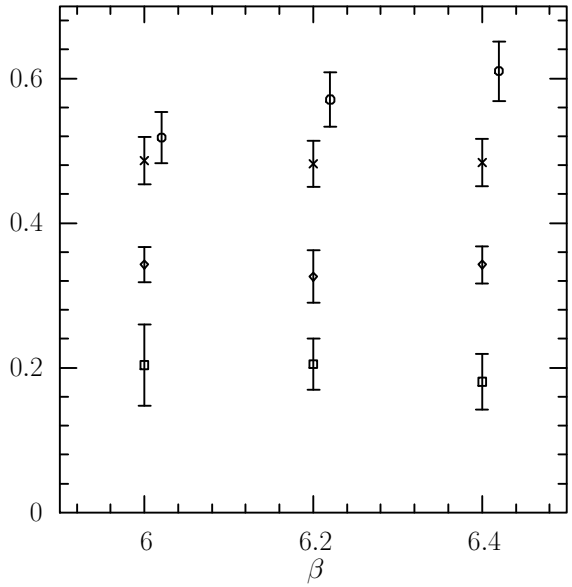

Figure 2. $\chi_t^{1/4}/\sqrt{\sigma}$ (circles), $\chi_t^{1/4}/(100\Lambda_{latt})$ (crosses), $\chi_t^{1/4}/m_\rho$ (diamonds), and $\chi_t^{1/4}/(10 f_\pi)$ (squares) versus β. Scaling is indicated when the ratios are independent of β. The actual values of these ratios are unimportant, since we consider only their dependence on β. The $16^3 \times 40$ lattice results are shown for $\beta = 6.0$.

embedded $SU(2)$ windings, we search for correlations between hypercubes of nonzero charge and plaquettes near the $SU(3)$ cut locus, the analog to the -1 group element in $SU(2)$. Plaquettes whose radial distance to cut locus (RDC)[13],

$$RDC = \left(2 \sum_{i=1}^{3} \theta_i^2 \right)^{1/2} \qquad (\frac{1}{\theta_3 - \theta_1} - \frac{1}{2\pi}) \qquad (4)$$

is less than 0.15 are selected for presentation here. In this definition (4) the θ_i are the three eigenangles of the $SU(3)$ matrix in ascending order, so that their sum is zero. For each charged hypercube in the ensemble the distance r_{min} from the center of the hypercube to the center of the nearest selected plaquette is found. The number of occurrences at each lattice distance r_{min}, $N(r_{min})$ is divided by the weight factor $g(r_{min})$, the number of available plaquettes at distance r_{min}, to obtain a normalized nearest neighbor correlation $n(r_{min})$. If the charges and nearly critical plaquettes are decoupled, $n(r_{min})$ will fall exponentially as a function of volume spanned by r_{min}, $n(r_{min}) \sim e^{-\alpha r^4_{min}}$.

As we investigate possible dislocations, we find some encouraging results. Our plot (Fig. 1) shows $n(r_{min})$ decaying exponentially as a function of r^4_{min}, except for a dramatic rise for $r_{min} < 2a$, indicating that questionable charges within $2a$ of a nearly critical plaquette may indeed be dominated by compact dislocations which are lattice artifacts. Where N_q is the number of questionable charges in a configuration, we find that $\langle N_q \rangle / \langle Q^2 \rangle = 0.21$ at $\beta = 6.0$, and 0.05 at $\beta = 6.4$. This decrease suggests that for the β values considered here the additive term in Eq. 3 is dominated by the $p > 0$ part of the integral, and

Table 1
Lattice Ensembles and Results

β	Lattice Size	Sample Size	$\chi_t^{1/4}(\sqrt{\sigma})$ (MeV)	$\chi_t^{1/4}(m_\rho)$ (MeV)
6.0	$16^3 \times 40$	34	228(15)	264(19)
6.0	$24^3 \times 40$	23	220(29)	255(34)
6.2	$32^3 \times 48$	22	251(16)	251(28)
6.4	$32^3 \times 48$	21	268(18)	264(20)

the divergent part $p < 0$ gives at most a negligible contribution to our measured χ_t. Also, as β increases, the physical charge is spread over a larger lattice volume and the short range peak of $n(r_{min})$ becomes more pronounced relative to the background exponential, allowing a cleaner filtering of dislocation-induced charges. Upon removing these charges we find that χ_t changes by about 1/3 of the statistical uncertainty for $\beta = 6.0$ and only about 1/10 of the uncertainty for $\beta = 6.4$. We take this as evidence that low-action dislocations have little effect on our measured susceptibility, and present results without removing questionable charges. The decrease of $\langle N_q \rangle / \langle Q^2 \rangle$ and the small effect of questionable charges on measured χ_t are also observed for other values of the *RDC* cutoff. A detailed analysis of the *RDC* cutoff will be presented in a forthcoming paper[14].

Since our calculation of χ_t spans a wide range of β we can check for scaling by plotting dimensionless ratios of $\chi_t^{1/4}$ to four other quantities versus β. Our computed values for $\chi_t^{1/4} a$ are 0.114(8) at $\beta = 6.0$ (16^3 lattice), 0.110(14) at $\beta = 6.0$ (24^3 lattice), 0.090(6) at $\beta = 6.2$, and 0.072(5) at $\beta = 6.4$. The height of each set of points is irrelevant since our concern is whether the ratios are independent of β. Scaling with m_ρ, f_π, and Λ_{latt} derived from the two-loop formula is apparent, but a possible slope exists in $\chi_t^{1/4}/\sqrt{\sigma}$. We present physical values derived from $m_\rho = 770\,\mathrm{MeV}$ and $\sqrt{\sigma} = 440\,\mathrm{MeV}$ in Table 1. Although the issue of scaling still must be resolved, we see that these results are consistent with earlier results by Göckeler *et al.*[12], computed on much smaller lattices. Consistency between the smaller and larger lattices at $\beta = 6.0$ indicates that our lattices are large enough to control finite size effects. We conclude that the geometric method yields χ_t about a factor of four higher than both the Witten-Veneziano prediction and the $\chi_t \approx (180\,\mathrm{MeV})^4$ obtained by cooling[7], and that the superficially divergent part of Eq. (3) is unlikely to cause this discrepancy.

Table 2
Lattice Observables (Lattice Units)

β	$\sigma^{1/2}a$	$m_\rho a$	$f_\pi a$
6.0	0.220(2)[1]	0.333(8)[3]	0.056(15)[3]
6.2	0.158(1)[1]	0.277(25)[2]	0.044(7)[2]
6.4	0.119(2)[1]	0.211(7)[4]	0.040(8)[4]

REFERENCES

[1] Schilling, K. and G. S. Bali, PRINT-93-0666 (Wuppertal), August 1993.

[2] C.R. Allton, *et al.* (The UKQCD Collaboration), EDINBURGH-92-507, June 1993.

[3] Cabasino, S. *et al.* (The APE Collaboration), *Phys. Lett.* **B258**, 195 (1991).

[4] Abada, A., *et al.*, *Nucl. Phys.* **B376**, 172 (1992).

[5] Di Vecchia, P., F. Nicodemi, R. Pettorino, and G. Veneziano, *Nucl. Phys.* **B181**, 318 (1981).

[6] Campostrini, M., A. Di Giacomo, H. Panagopoulos, and E. Vicari, *Nucl. Phys.* **B329**, 683 (1990).

[7] Teper, M., *Phys. Lett.* **B202**, 553 (1988).

[8] Teper, M., *Phys. Lett.* **B232**, 227 (1989).

[9] Lüscher, M., *Commun. Math. Phys.* **85**, 39 (1982).

[10] Kremer, M., A. S. Kronfeld, M. L. Laursen, C. Schierholz, C. Schleiermacher, U. -J. Wiese, *Nucl. Phys.* **B305**, 109 (1988).

[11] Göckeler, M., A. S. Kronfeld, M. L. Laursen, G. Schierholz, and U. -J. Wiese, *Phys. Lett.* **B233**, 192 (1989).

[12] Göckeler, M., A. S. Kronfeld, M. L. Laursen, G. Schierholz, and U. -J. Wiese, *Nucl. Phys.* **B292**, 349 (1987).

[13] Lasher, G., *Nucl. Phys.* B *(Proc. Suppl.)* 9, 416 (1989).

[14] Grandy, J., and R. Gupta (in progress).